

## P2M.11 Disdrometer and Radar Observation-Based Microphysical Parameterization to Improve Weather Forecast

Guifu Zhang<sup>+</sup>, Juanzhen Sun<sup>\*</sup>, Edward Brandes<sup>\*</sup>, Jimy Dudhia<sup>\*</sup>, and Wei Wang<sup>\*</sup>

<sup>+</sup>: School of Meteorology, University of Oklahoma, Norman, OK 73019

<sup>\*</sup>: National Center for Atmospheric Research, Boulder, CO 80307-3000

### 1. Introduction

The fundamental characterization of rain microphysics is through the raindrop size distribution (DSD). Microphysical processes of evaporation, accretion, and precipitation rate are all related by the DSD. Most parameterization schemes used in numerical weather prediction were developed (Kessler, 1969) on the assumption of an exponential distribution of raindrops, written as

$$N(D) = N_0 \exp(-\Lambda D), \quad (1)$$

where the slope parameter  $\Lambda$  relates to a characteristic size of the raindrops such as the mean diameter ( $\langle D \rangle$ ) or median volume diameter ( $D_0$ ).  $N_0$  is an intercept parameter, which was fixed at  $10000 \text{ m}^{-3} \text{ mm}^{-1}$  by Kessler. When  $N_0 = 8000 \text{ m}^{-3} \text{ mm}^{-1}$ , Eq. (1) becomes the Marshall–Palmer (M-P) drop size distribution (Marshall and Palmer, 1948). For the M-P DSD model and Kessler's parameterization scheme, microphysical processes for evaporation rate ( $R_e$  in  $\text{g m}^{-3} \text{ s}^{-1}$ ) for a unit water vapor saturation deficit, accretion rate ( $R_c$  in  $\text{g m}^{-3} \text{ s}^{-1}$ ) for a unit cloud water content, and mass-weighted terminal velocity ( $V_{tm}$  in  $\text{m s}^{-1}$ ) can be represented in terms of rain water content ( $W$  in  $\text{g m}^{-3}$ ) as follows

$$R_e = 5.03 \times 10^{-4} W^{13/20} \quad (2)$$

$$R_c = 5.08 \times 10^{-3} W^{7/8} \quad (3)$$

$$V_{tm} = 5.32 W^{1/8} \quad (4)$$

The radar reflectivity factor at horizontal polarization ( $Z_H$  in  $\text{mm}^6 \text{ m}^{-3}$ ) is related to water content by

$$Z_H = 2.04 \times 10^4 W^{7/4} \quad (5)$$

Although there have been some modifications, e.g., Klemp and Wilhelmson (1978), and Lin et al. (1983), this simple approach to model parameterization, called a Kessler-type scheme, is still widely used in mesoscale models. The problem with fixed-intercept parameterizations is that the rain water gets redistributed into smaller drop categories as the drop spectra slope parameter increases, thus accelerating the process of rain water removal through evaporation. Rainfall rate cannot be accurately estimated with a  $R$ - $Z$  relation derived from the M-P DSD model (Wilson and Brandes 1979), having estimation error of 50%. Another issue with the M-P model is the convergence problem which occurs in a four-dimensional data assimilation (4D-Var) system, due to the highly nonlinear nature of expressions such as Eqs (2) and (4), the minimization of the cost function tends to have convergence problems (Sun and Crook, 1997).

---

*Corresponding author address:* School of Meteorology, University of Oklahoma, Norman, OK 73019;  
Email: guzhang1@ou.edu

The gamma distribution has been used to improve the characterization of rain DSDs over the exponential distribution (Ulbrich, 1983). Recent disdrometer observations indicate that rain DSDs can be represented by a constrained-gamma (C-G) distribution model (Zhang et al. 2001). The C-G model was developed for retrieving rain DSDs from polarization radar observations. The procedure is to determine the three parameters of the gamma distribution from radar reflectivity, differential reflectivity, and a constraining relation between the shape and slope of the distribution. It has been shown that the C-G model characterizes natural DSDs better and leads to more accurate retrievals than that with a two parameter exponential model and with a variable  $N_0$  (Brandes et al. 2003). The C-G rain DSD model allows accurate rainfall estimation and detailed study of storm microphysics (Brandes et al., 2005; Zhang et al., 2005).

In this paper, we apply the constrained-gamma DSD model to the microphysical parameterization in a cloud model and evaluate the impact of the parameterization scheme on the initialization and forecasting of storms

### 2. Parameterization of rain microphysics based on constrained-gamma DSD model

The constrained-gamma DSD model consists of a gamma distribution in the form (Ulbrich, 1983)

$$N(D) = N_0 D^\mu \exp(-\Lambda D) \quad (6)$$

[where  $N_0$  ( $\text{mm}^{-1-\mu} \text{ m}^{-3}$ ) is a concentration parameter,  $\mu$  is a shape parameter, and  $\Lambda$  ( $\text{mm}^{-1}$ ) is a slope parameter] and a constraining relation between  $\mu$  and  $\Lambda$  given by

$$\Lambda = 0.0365 \mu^2 + 0.735 \mu + 1.935 \quad (7)$$

Relation (7) was derived from 2-D video-disdrometer measurements made in Florida (Zhang et al. 2001) and has been verified by data collected in Oklahoma (Brandes et al. 2003). It has been shown that (7) characterizes natural rain DSD variations quite well and applies to both convective and stratiform DSDs except for that at leading edges of convective storms and drizzle rains. Fine tuning for geographical locations/climatology with further observations may improve the model results.

The constrained-gamma DSD model represented by (6) and (7) is essentially a two-parameter model much like the exponential distribution or a gamma distribution with a fixed  $\mu$ . The difference, however, is that the constrained-gamma DSD model is capable of describing a variety of drop-size distributions with different spectral shapes: concave upward shape for a broad distribution versus convex for a narrow distribution on a semi-logarithm plot. Because  $\mu$  and  $\Lambda$  jointly describe the DSD shape, the characteristic size (e.g.,

median volume diameter  $D_0$ ) and the spectrum width are related. This makes physical sense because, except at the leading edge of some convective storms, large raindrops are usually accompanied by small drops, which leads to a broad spectrum. On the other hand, small and medium size raindrops are not necessarily accompanied by large drops, e.g., stratiform and light convective rain DSDs. A  $\mu - \Lambda$  (or  $\mu - D_0$ ) relation allows better characterization of the raindrop size/spectrum width dependence than a fixed distribution shape without increasing the number of parameters. A fixed  $\mu$  is a special  $\mu - \Lambda$  relation, e.g.; an exponential distribution ( $\mu = 0$ ).

The  $\mu - \Lambda$  relation facilitates the reliable retrieval of the gamma DSD parameters ( $N_0$ ,  $\mu$ , and  $\Lambda$ ) from polarization radar measurements of radar reflectivity factor ( $Z_H$ ) and differential reflectivity ( $Z_{DR}$ ). Once the rain DSD is known, rain microphysical processes can be estimated. The constrained- gamma DSD model with two independent parameters can be used to derive rain physical parameter and microphysical processes: water content ( $W$  in  $\text{g m}^{-3}$ ), evaporation rate ( $R_e$  in  $\text{g m}^{-3} \text{s}^{-1}$ ), accretion rate ( $R_c$  in  $\text{g m}^{-3} \text{s}^{-1}$ ) and mass-weighted terminal velocity ( $V_{tm}$  in  $\text{m s}^{-1}$ ) Following Kessler's parameterization procedure, the microphysical process parameters are derived (Zhang et al., 2005) by integration of the gamma DSD (6).

For convenience, the C-G parameterization are expressed in terms of  $Z_H$  and  $Z_{DR}$  as

$$W = Z_H \times 10^{(0.229Z_{DR}^2 - 1.212Z_{DR} - 3.232)} \quad (8)$$

$$R_e = Z_H \times 10^{(0.322Z_{DR}^2 - 1.649Z_{DR} - 6.298)} \quad (9)$$

$$R_c = Z_H \times 10^{(0.238Z_{DR}^2 - 1.293Z_{DR} - 5.448)} \quad (10)$$

$$V_{tm} = -0.592Z_{DR}^2 + 2.870Z_{DR} + 3.573 \quad (11)$$

Eqs. (8)-(11) are obtained by fitting  $W/Z_H$ ,  $R_e/Z_H$ ,  $R_c/Z_H$  and  $V_{tm}$  to polynomial functions of  $Z_{DR}$ . The fitting results are shown in Fig. 1. The discrete points are calculations from disdrometer data collected in east-central Florida during the summer of 1998 field program (PRECIP98) (Zhang et al. 2001; Brandes et al. 2003). The ratios  $R_e/Z_H$  and  $R_c/Z_H$  decrease as  $Z_{DR}$  increases except for  $R_e/Z_H$  at large  $Z_{DR}$  because  $Z_{DR}$  is related to droplet size and the total surface area and cross section associated with evaporation and accretion are smaller for DSDs dominated by large raindrops (large  $Z_{DR}$ ) than for small drops at the same  $Z_H$ . The flattening of  $R_e/Z_H$  at large  $Z_{DR}$  is due to the fact that large  $Z_{DR}$ s usually occur in storm centers where DSDs typically have a broad distribution with large numbers of small drops.

### 3. Simplified constrained-gamma model parameterization

Bulk model parameterization in most numerical simulations using the M-P DSD model is typically based on only one parameter, liquid water content or water mixing ratio. To apply the C-G model parameterization, (8)-(11), in a bulk model, we need to reduce the two-parameter model to a single parameter. It is noted that for rain the radar measurements of reflectivity and differential reflectivity are *statistically* related. Analysis of the PRECIP98 dataset leads a mean relation (Zhang et al. 2005)

$$Z_{DR} = 10^{(-2.362 \times 10^{-4} Z_H^2 + 0.04581 Z_H - 1.4333)}, \quad (12)$$

where  $Z_H$  is in dBZ and  $Z_{DR}$  is in dB.

Based radar retrieval, the microphysical process parameters are expressed as function of rain water content as

$$R_e = 10^{(0.00679(\log W)^4 + 0.0557(\log W)^3 + 0.119(\log W)^2 + 0.937\log W - 3.369)} \quad (13)$$

$$R_c = 10^{(-0.0000603(\log W)^4 - 0.00255(\log W)^3 - 0.0212(\log W)^2 + 0.933\log W - 2.294)} \quad (14)$$

$$V_{tm} = -4.509 \times 10^{-4} (\log W)^4 + 0.0148(\log W)^3 + 0.263(\log W)^2 + 1.410\log W + 5.799 \quad (15)$$

The simplified C-G (S-C-G) parameterization scheme of (13)-(15) can be applied to any numerical weather model with microphysics characterized by a *single parameter*, that is, by bulk water content or rain water mixing ratio. Rain water estimates from radar reflectivity using the S-C-G model with (8) and (12) and the M-P model (5) are compared in Fig. 2. Calculations with disdrometer data are also shown for reference. It is seen that the two estimated water contents agree for the medial radar reflectivity values at which most rain falls, but the S-C-G DSD model allows a larger dynamic range of water content and gives a smaller water content for weak radar reflectivity (stratiform rain) than the M-P model. The S-C-G model results agree with disdrometer observations better than the M-P model.

Figure 3 shows the spatial distributions of the rain microphysical process parameters estimated from NCAR's Spol radar measurements using the C-G, S-C-G, and M-P models. The polarization radar is located at (-9km, -25km) from the origin. The radar measurements of reflectivity and differential reflectivity were collected at 0.5 degree of elevation. In general, the C-G model gives a larger dynamic range, and more detailed features, and larger spatial variations for  $R_e$  and  $R_c$  than the M-P model. Results for the S-C-G model are between that for the C-G and M-P models. The M-P model overestimates evaporation by about three times for the stratiform rain in the upper-right corner of the images. The S-C-G model gives stratiform rain evaporation close to that of the C-G model.

### 4. Application of the S-C-G parameterization in model forecasting

The parameterization scheme (13)-(15) was implemented in the warm cloud model (Sun and Crook, 1997) and the Weather Research Forecast (WRF) model (Hong et al. 2004). The cloud model, Variational Doppler Radar Analysis System (VDRAS), is chosen for our study because it has a 4D-Var radar data assimilation system for model initialization.

The simulation domain with the VDRAS is a region of  $140 \times 140 \times 15 \text{ km}^3$  with  $70 \times 70 \times 30$  grid points. The cloud model is initialized by assimilating radar data from the Melbourne, Florida WSR-88D (KMLB). Thunderstorms examined here formed in central Florida on 2 September as part of an outer rainband associated with hurricane Earl. Three volumetric datasets at 2310, 2315, and 2320 UTC, when the storms were most intense, are used for model initialization with the 4D-Var technique. Radar reflectivities ( $Z_H > 5 \text{ dBZ}$ ) were converted to rain water contents using (8) and (12) for the S-C-G model and (5) for the M-P model. The first guess (and background) of the 4D-Var data assimilation is from a sounding released at 1900.

The initial conditions were found iteratively until a step change of the cost function fell below a threshold value. It took 117/105 iterations for the S-C-G/M-P models. The initial condition from the 4D-Var was then used to make forecasts with S-C-G and M-P microphysical parameterizations. Fig. 4 shows comparisons of rain water content estimated from radar measurements and model results at the first level for 30-min forecast (2350 UTC). The forecast results are shown by a threshold of  $W > 0.001 \text{ g m}^{-3}$ . The up-left panel is the water content estimated from polarization radar (S-Pol) measurements of  $Z$  and  $Z_{DR}$  using Eq. (8). The up-right is reflectivity-based rain water estimates from KMLB radar with Eq. (5). The S-C-G model forecasted water contents are consistent with the S-Pol radar estimates from reflectivity and differential reflectivity. The M-P model results do not agree with radar estimates from either dual-polarization measurements or reflectivity only. Clearly, the S-C-G forecasts agree with radar estimates better than the M-P model in terms of both coverage and intensity.

The model rain water contents are converted to radar reflectivities by solving inversion problems of (8) and (12) for S-C-G model and (5) for the M-P model (using the two curves in Fig. 2). Fig. 5 shows the reflectivity results for the initialization time (2320 UTC) and for 30-minute forecasts (2350 UTC, respectively). The retrieved wind field at the initialization time and the forecast wind are overlaid on the reflectivity field. The left (right) column presents results for the S-C-G model (M-P model) parameterization. The radar observations are shown in the middle column for comparison. Fig. 5a is the results at the first model level (0.25 km above ground).

Our results suggest that the S-C-G model parameterization has several advantages over the M-P DSD model. Stratiform precipitation in the upper-right corner is better represented in the model initialization and is better preserved in the forecasts. This is because the S-C-G parameterization leads to smaller evaporation and accretion rates, as discussed in the previous section. Also, the linearity at low evaporation (a constant derivative) with the S-C-G model allows better convergence in the minimization and a more accurate fit with observations. The S-C-G model forecasts of convective cores (intensity) agree with radar observations better than the M-P model. The M-P model tends to over-predict rain intensity in the storm core while under-forecasting the total storm coverage due to a rapid decay of the stratiform rain. The difference in the predicted reflectivity values is due to over-predicted water contents by the M-P model and different  $W$ - $Z$  relations used in the S-C-G and M-P model. Perhaps this is a result of higher evaporation in convective storm cores with the S-C-G model.

To show the vertical structure of the storm, results at  $y = -30$  km at initialization and for 30-minute forecasts in Fig. 5b are plotted. A radar bright-band was not evident in this warm rain system. Both the S-C-G and M-P model initializations have background residual precipitation in the left-hand portions of the images, but the S-C-G model initialization and forecasts agree with observations better than the M-P model for rain aloft and near the ground. The high evaporation rate in the M-P model parameterization causes fast decay of rain with low water content and prevents some stratiform rain

from reaching the ground. The S-C-G model results are more accurate and reasonable in characterizing the spatial precipitation distribution and storm evolution than the M-P model.

Figure 6 shows a preliminary study with WRF model. The WRF single moment 6-class (WSM6) scheme is modified to accommodate the S-C-G model for rain terms. A 2-dimensional simulation of a squall line was ran with WRF and shown in the figure. The forecasts using the S-C-G model and M-P model are different. Further study such as modification to ice/mixed-phase microphysics is needed to see the impact of observation-based model parameterization on numerical forecast.

## 5. Summary and discussion

This paper presents a parameterization scheme for rain microphysical processes based on a constrained-gamma DSD model developed from disdrometer and polarization radar observations. The C-G DSD model yields smaller evaporation and accretion rates as well as their derivatives than the M-P model for stratiform rain, and higher  $R_e$  and  $R_c$  in the core regions of convective storms. The C-G model parameterization was further simplified to a single-parameter scheme (S-C-G) in which the microphysical process parameters are expressed by polynomial functions of rain water content. The exponent polynomial form has better performance (continuity and linearity) at lower water contents than the power-law form of the M-P model. The S-C-G model parameterization produces better variational analysis for model initialization and better short-term forecasts for warm rain processes by (i) preserving the stratiform component of the precipitation and (ii) predicting the intensity of convective cores more accurately than M-P model parameterization. This is because the S-C-G model yields less (more) evaporation and accretion than the M-P model at low (high) rain water content.

Accurate microphysical parameterization based on advanced measurement techniques such as polarization radar observations and disdrometer measurements is highly desirable and feasible. Because radar provides large coverage weather observations and a 2-D video disdrometer measures “ground-truth”, a combination of polarization radar and disdrometer measurements makes observation-based model parameterization reliable and useful. Future work will be on applying the C-G parameterization to a two-moment numerical weather model so that both radar reflectivity and differential reflectivity are used to characterize rain microphysics, to initialize the model, and to verify the forecast.

## Acknowledgements

The research was supported by NCAR Director’s Opportunity Fund and by funds from the National Science Foundation that have been designated for U.S. Weather Research Program activities at the National Center for Atmospheric Research (NCAR). We sincerely appreciate helpful discussions with Ms. Ying Zhang, Drs. Frederick H. Carr, Kelvin K. Droegemeier, Jerry Straka, and Ming Xue.

## REFERENCES

- Brandes, E. A., G. Zhang, and J. Vivekanandan, 2003: An evaluation of a drop distribution-based polarimetric radar rainfall estimator. *J. Appl. Meteor.*, **42**, 652–660.
- Brandes, E. A., G. Zhang, and J. Sun, 2005: On the influence of assumed drop size distribution form on retrieved thunderstorm microphysics. Submitted to *J. Appl. Meteor.*.
- Chen, J.-P., and S.-T. Liu, 2004: Physically based two-moment bulkwater parameterization for warm-cloud microphysics. *Quart. J. Roy. Meteor. Soc.*, **130**, 51–78.
- Hong, S.-Y., J. Dudhia, and S.-H. Chen, 2004: A revised approach to ice microphysical processes for the bulk parameterization of clouds and precipitation. *Mon. Wea. Rev.*, **132**, 103–120.
- Kessler, E., 1969: On the distribution and continuity of water substance in atmospheric circulations. *Meteor. Monogr.*, No. 32, Amer. Meteor. Soc., 84 pp.
- Klemp, J. B., and R. B. Wilhelmson, 1978: The simulation of three-dimensional convective storm dynamics. *J. Atmos. Sci.*, **35**, 1070–1096.
- Lin, Y.-L., R. D. Farley, and H. D. Orville, 1983: Bulk parameterization of the snow field in a cloud model. *J. Climate Appl. Meteor.*, **22**, 1065–1092.
- Marshall, J.S., and W. McK. Palmer, 1948: The distribution of raindrops with size, *J. Meteor.*, **5**, 165–166.
- Sun, J., and N. A. Crook, 1997: Dynamical and microphysical retrieval from Doppler radar observations using a cloud model and its adjoint. Part I: Model development and simulated data experiments. *J. Atmos. Sci.*, **54**, 1642–1661.
- Ulbrich, C.W., 1983: Natural variations in the analytical form of the raindrop size distribution, *J. Appl. Meteor.*, **22**, 1764–1775.
- Zhang, G., J. Vivekanandan, and E. Brandes, 2001: A method for estimating rain rate and drop size distribution from polarimetric radar measurements. *IEEE Trans. Geosci. Remote Sens.*, **39**, 830–841.
- Zhang, G., J. Sun, and E. Brandes, Improving parameterization of rain microphysics with disdrometer and radar observation, Submitted to *J. Atmos. Sci.*, 2005.

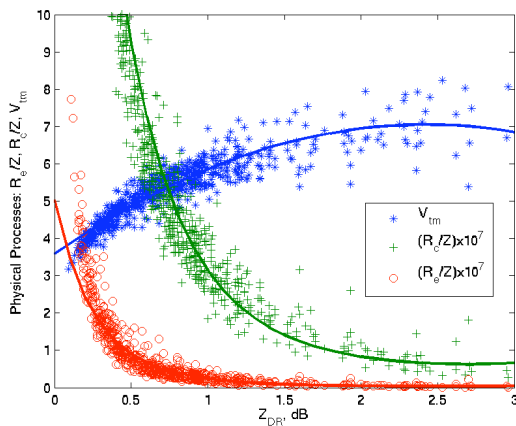


Fig. 1: Dependence of rain microphysical process parameters ( $R_e$ ,  $R_c$ , and  $V_{tm}$ ) on median volume diameter ( $D_0$ ) for constrained-gamma (C-G) DSDs. The discrete points are estimates from disdrometer measurements.  $R_e$  and  $R_c$  are in  $\text{g m}^{-3} \text{ s}^{-1}$ ,  $W$  in  $\text{g m}^{-3}$  and  $V_{tm}$  in  $\text{m s}^{-1}$ .

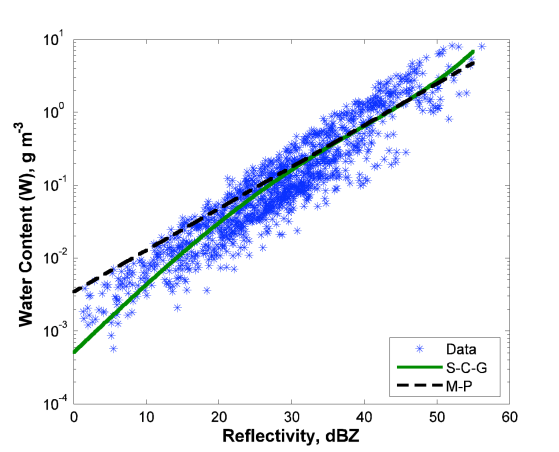


Fig. 2: Comparison of rain water content estimates using the simplified constrained-gamma (S-C-G) and Marshall-Palmer (M-P) DSD models.

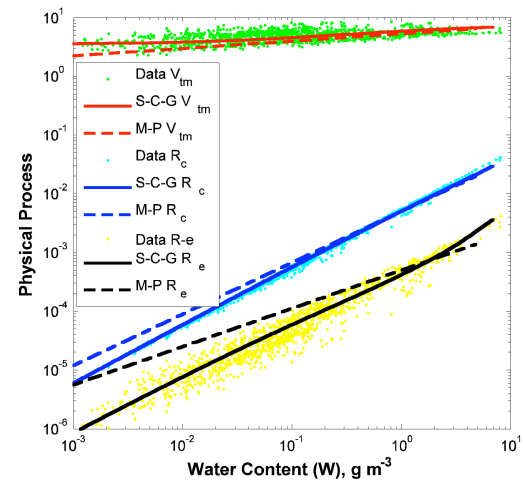


Fig. 3: Comparison of rain physical process parameters between S-C-G DSD and M-P DSD model.  $R_e$  and  $R_c$  are in  $\text{g m}^{-3} \text{ s}^{-1}$ , and  $V_{tm}$  in  $\text{m s}^{-1}$ .

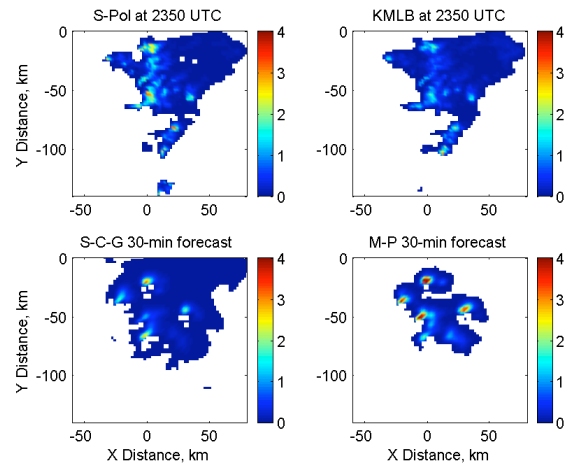
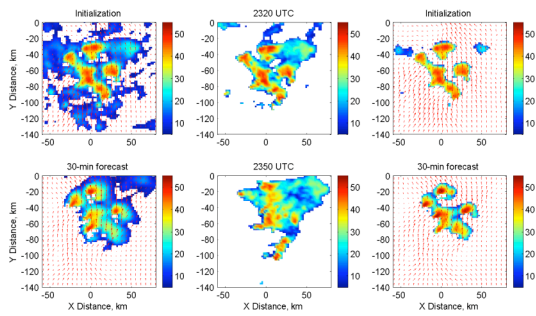
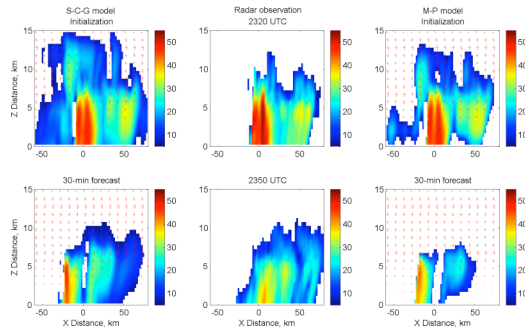


Fig. 4: Comparison of rain water content ( $\text{g m}^{-3}$ ) between radar estimates and model forecasts for the first level at 2350 UTC (30-min forecast).



(a)



(b)

Fig. 5: Comparison of reflectivity factors of numerical weather forecasts based on the S-C-G (left column) and M-P (right column) model parameterizations as well as radar observation (middle column). Rows show the model and observed reflectivity at initialization (2320 UTC) and for 30-minute forecasts (2335, and 2350 UTC). (a) first level.; (b) vertical profiles at  $y = 30\text{km}$ .

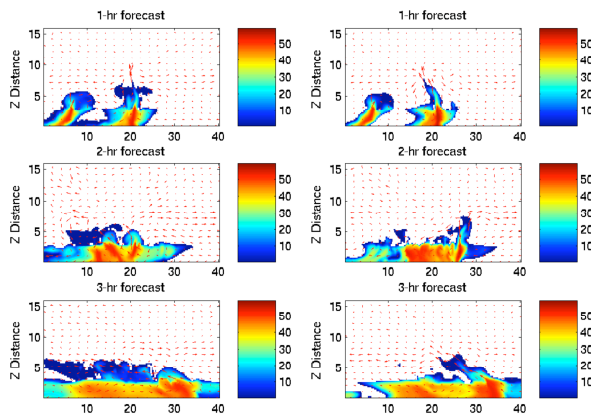


Figure 6: Simulations of 2D squalline with WRF model using parameterization schemes associated with S-C-G and M-P DSD model.